

Resistivity Imaging of the Santa Maria Sector and the Northern Zone of Las Pailas Geothermal Area in Costa Rica by using Joint 1D Inversion of TDEM and MT Data

Diego Badilla Elizondo

101 Reykjavik, Iceland

dabe@unugtp.is

Keywords: resistivity, magnetotellurics, TDEM, Santa Maria, deep conductor, Rincon de la Vieja

ABSTRACT

Geophysical exploration surveys were carried out by using MT and TDEM methods in the northeastern sector of Las Pailas Geothermal area. The electrical resistivity of the subsurface was modelled and interpreted for two specific areas located to the north and east of Las Pailas Geothermal Field in Costa Rica. The static shift problem of MT data was solved by inverting jointly both TDEM and MT soundings. Seven geophysical profiles were analysed based on 1D models from 22 MT and 19 TDEM soundings. Resistivity cross sections and iso-resistivity maps were compiled. We were aiming to image anomalies that could help to understand the conceptual model thinking in the future expansion of the actual production field. The different stages of alteration mineralogy were mapped and they are directly associated with the main geothermal signatures of a high temperature geothermal field. It was confirmed the existence of a structure trending probably NW-SE in the northern side of the survey area and in Santa Maria sector. A low resistivity body (deep conductor) was also mapped to the northern part of the study area which probably represent the heat source for the field.

1. INTRODUCTION

Geophysical exploration methods for geothermal resources is an essential tool. By combining together with geochemistry and geology it can give a good contribution before the drilling stage to reduce the risk associated to uncertainties of the conceptual models. Resistivity is directly related to the properties of interest for geothermal exploration as temperature, porosity (permeability) and alteration. To a great extent, these parameters characterize the reservoir (Hersir and Árnason, 2009). This capacity of the resistivity has made from the electromagnetic methods one of the most powerful tools in geothermal exploration.

In this work we used electromagnetic data from magnetotellurics (MT) and transient electromagnetics (TEM) to create a resistivity model that could contribute to clarify and explain the presence (or not) of the main anomalies related to signatures of a high temperature geothermal field the sector of Santa Maria and northeast from Las Pailas GF. The work was done in 2011 as part of the UNU- geothermal training program in Iceland, where we had the supervision of ÍSOR (Iceland Geosurvey) experts.

Las Pailas Geothermal Area is located on the southern flank of the Rincón de la Vieja Volcano. It belongs to the Guanacaste volcanic range and is located between the Miravalles and Orosí volcanoes. Las Pailas Geothermal Field is producing 35 MWe since 2011 and increased its production in 55 MWe in June, 2019, for a total of 90 MWe. It means the country is generating a total of ~253 MWe from geothermal and that corresponds to a contribution of ~16 of the total energy required.

1.1 Geology

Rincon de la Vieja is a composite stratovolcano located in the northwestern part of Costa Rica, in the Guanacaste Volcanic Range and forms a northwest trending ridge consisting of several eruptive centres (Kempster, 1997).

2. METHODS

2.1 The MT method

The magnetotelluric (MT) method involves measuring the fluctuations in the earth natural electric (**E**) and magnetic (**B**) fields in orthogonal directions on the surface. It is a mean to determine the resistivity structure of the earth at depths ranging from a few tens of meters down to several hundreds of kilometres (Simpson and Bahr, 2005). The impedance tensor relates the orthogonal components of the horizontal electric and magnetic fields:

$$\begin{bmatrix} E_x \\ E_y \end{bmatrix} = \begin{bmatrix} Z_{xx} & Z_{xy} \\ Z_{yx} & Z_{yy} \end{bmatrix} \begin{bmatrix} H_x \\ H_y \end{bmatrix} \quad (1)$$

or

$$E_x = Z_{xx}H_x + Z_{xy}H_y \quad (2)$$

$$E_y = Z_{yx}H_x + Z_{yy}H_y \quad (3)$$

Resistivity can be expressed as the ratio of the orthogonal electric, **E**, and magnetic, **B**, fields as a function of the period T, given by equation (4):

$$\rho = \frac{1}{\omega\mu} \left| \frac{\mathbf{E}}{\mathbf{H}} \right|^2 = 0.2T \left| \frac{\mathbf{E}'}{\mathbf{B}'} \right|^2 \quad (4)$$

where,

ω = Angular frequency ($2\pi f$);

μ = Magnetic permeability (H/m);

\mathbf{E} = Electrical field (V/m);

\mathbf{H} = Magnetic field intensity (T);

\mathbf{E}' = Electrical field (mV/km);

\mathbf{B}' = Magnetic field (nT), $\mathbf{B}' = \frac{\mu \mathbf{H}}{10^{-9}}$;

1D earth case

For a 1D layered earth, the conductivity varies only with depth and consequently the diagonal elements of the impedance tensor presented in equation (1) Z_{xx} and Z_{yy} are zero. Those diagonal elements couple parallel electric and magnetic field components. Whilst the off-diagonal components (which couple orthogonal electric and magnetic field components) are equal in magnitude, but have opposite signs. The impedance tensor \mathbf{Z} can be written as:

$$\mathbf{Z} = \begin{bmatrix} 0 & Z_{xy} \\ Z_{yx} & 0 \end{bmatrix} \quad (5)$$

Where, $Z_{xy} = -Z_{yx} \neq 0$

For a homogeneous earth the orthogonal impedance tensor components can be related and expressed as:

$$Z_{xy} = \frac{E_x}{H_y} = \frac{i\omega\mu}{k} = \sqrt{\frac{\omega\mu}{\sigma}} e^{i\pi/4} \quad (6)$$

$$Z_{yx} = \frac{E_y}{H_x} = \frac{-i\omega\mu}{k} = -Z_{xy} \quad (7)$$

Equations (6) and (7) have a constant phase of $\theta = \pi/4$; the magnetic field is 45° behind the electric field. We can calculate the resistivity of the half space by:

$$\rho = \frac{1}{\omega\mu} |Z_{xy}|^2 = \frac{1}{\omega\mu} |Z_{yx}|^2 \quad [\Omega m] \quad (8)$$

2.2 The TEM method

The Transient Electromagnetic (TEM) method, also known as Time Domain Electromagnetics (TDEM) is an exploration technique used to obtain the subsurface resistivity information, from a few metres to less than 1 km. A typical TEM sounding survey configuration is the central loop (see Figure 1). Here, a transmitter is connected to a square loop of wire that was placed on the surface and a multi turn receiver coil, located at the centre of the transmitter loop is connected to the receiver. A magnetic field of known strength is built up by transmitting a periodic and symmetrical current signal into the loop (Kaufman and Keller, 1983)

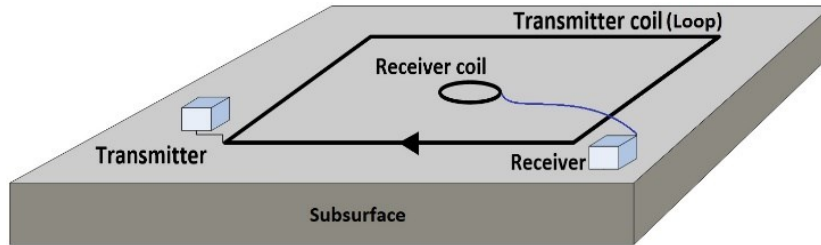


Figure 1: Typical central loop TDEM configuration (modified from Phoenix Geophysics, 2015)

The current distribution and the decay rate of the secondary magnetic field created in the subsurface depend on the resistivity structure of the earth. The decay rate, recorded as a function of time (time gates) just after the current in the transmitter loop goes to zero can therefore be interpreted in terms of the subsurface resistivity structure (Arnasón, 1989).

3. ELECTROMAGNETIC SURVEY

The study area is presented in Figure 2. The resulting profiles and associated electromagnetic soundings, the first production wells and the boundary of the Rincon de la Vieja National Park are marked. First, the survey was performed for the MT data collection and after that the TDEM campaign. 22 MT and 19 TDEM sounding data were collected.

The MT data were acquired using the configuration from Phoenix Geophysics (2015). Five channels were recorded, two for the electric field (Ex, Ey) and three for the magnetic field (Hx, Hy, Hz). The magnetotelluric data were collected for frequencies ranging from 400 Hz to 0.0001 Hz.

In the TDEM campaign, a typical central loop field configuration was used (see Phoenix Geophysics, 2015). A single turn 100 m by 100 m or two turns 50 m by 50 m side transmitter loop was used depending on topography. Data were collected for two different frequencies (30 and 5 Hz). The acquisition time was in average 15 min.

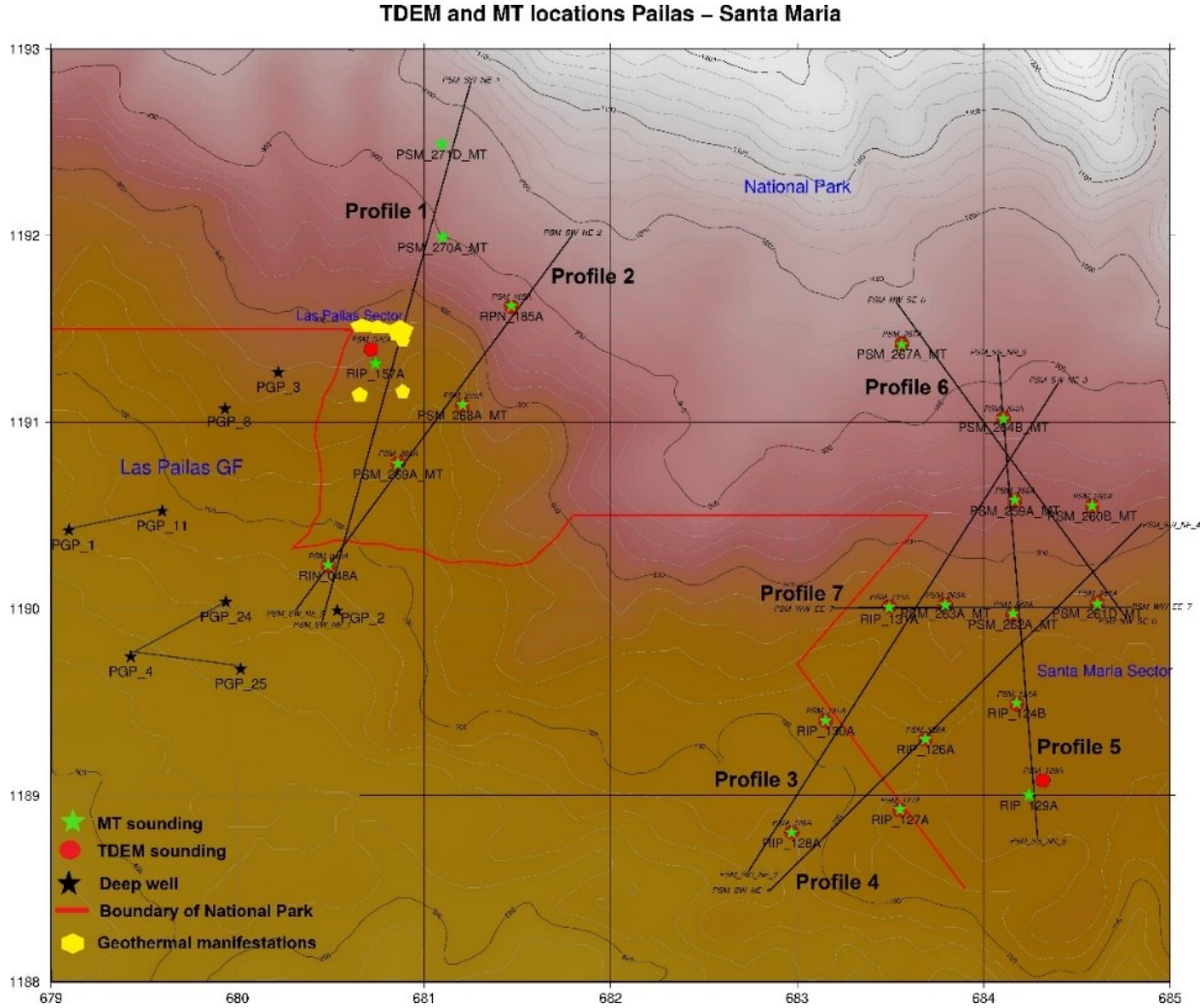


Figure 2: Location map of the study area showing in green the location of the MT soundings and in red TDEM sites. Coordinates are in UTM-Z16 (km)

3. DATA PROCESSING AND INVERSION

The resistivity is calculated using the method of the determinant of the impedance tensor, which is rotationally invariant. The determinant value is calculated as shown in equation (6):

$$\rho_{det} = \frac{1}{\omega\mu} |Z_{det}|^2 = \frac{1}{\omega\mu} |\sqrt{Z_{xx}Z_{yy} - Z_{xy}Z_{yx}}|^2; \quad \theta_{det} = \arg(Z_{det}) \quad (6)$$

The MT and DC methods which are based on measuring the electric field (**E**) on the surface suffer the static shift problem. Static shift can be caused by any multi-dimensional conductivity contrasts (superficial in-homogeneities) that can considerably affect the results. The causes of the static shift distortion are: electric field distortion due to lateral discontinuities, current channeling/repelling and topographic effects.

3.1 Joint 1D inversion of MT and TDEM

In the joint inversion the TDEM soundings are used to correct for the static shift problem of the MT stations as they are relatively unaffected by the superficial and lateral distortions. In Figure 3 we show how the MT sounding (blue squares) is tied in to the TDEM sounding (red diamonds) and the best fitting curve for both is obtained at the same time giving the solution of the smooth resistivity model as shown to the right. The static shift multiplier is 0.528 in this case and the fitting error is represented by the RMS = 1.016.

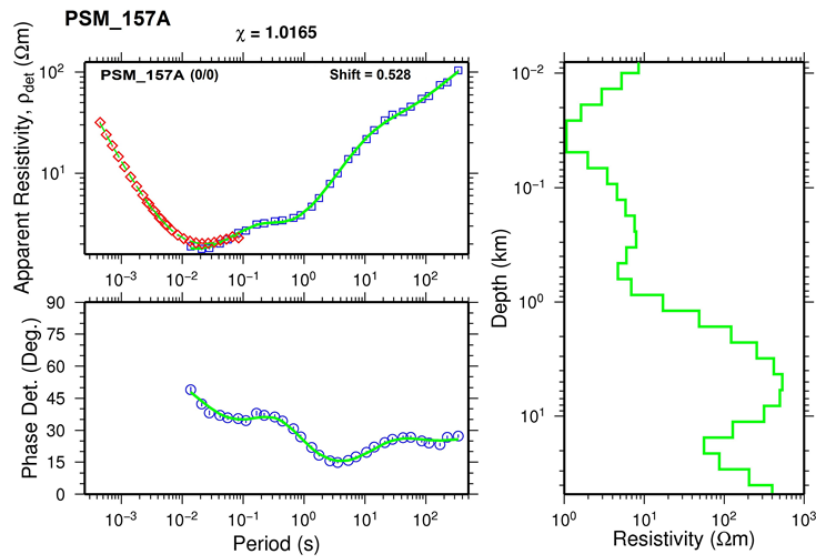


Figure 3: Result of a joint 1D inversion of TDEM and MT soundings. Red diamonds represent the TDEM apparent resistivities transformed to a pseudo-MT curve (Sternberg et al., 1988); the blue squares and circles are the measured apparent resistivity and phase derived from the determinant of MT impedance tensor

3. RESULTS AND DISCUSSION

The geoelectrical strike based on the impedance for intermediate/great depths is presented in Figure 4. A trend NW-SE is well defined probably associated to strike slip faulting systems (DeMets, 2001; Arias, 2002; Climent et al., 2014).

Z strike distribution 1–1000 s

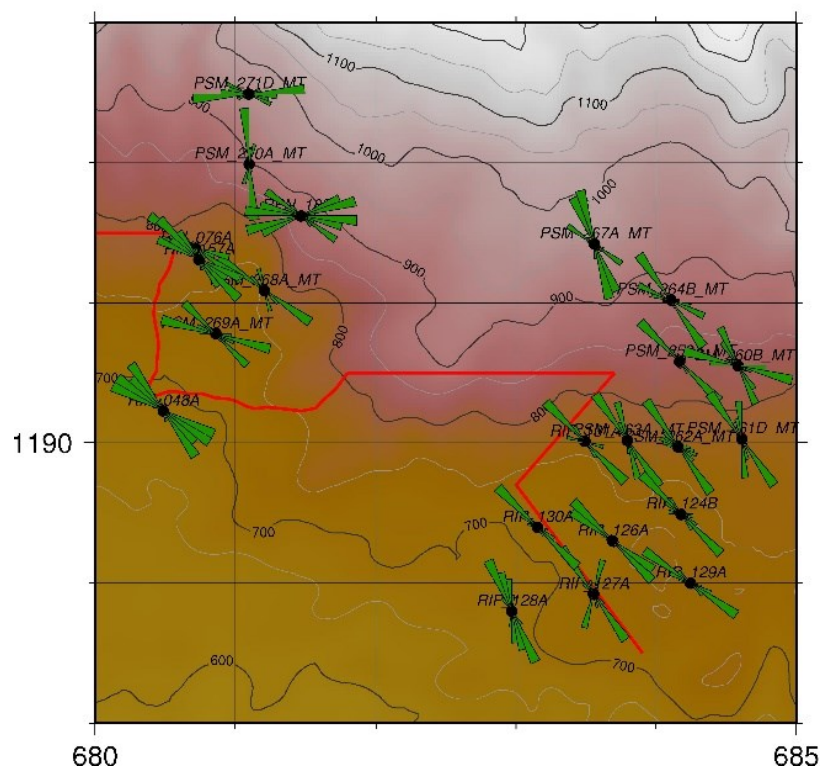


Figure 4: Geoelectrical strike based on Zstrike for the periods from 1 to 1000 s. Black dots denote MT soundings. Red line marks the national park boundary. Coordinates in UTM-Z16(km)

A well-defined low resistivity layer (1 to 10 Ωm) is present in all the cross sections. It is interpreted as the smectite clay cap and related to temperatures between 100°C and 220°C. It is possible to see low resistivity in the very shallow part and around the sounding

RIP_157A (PSM_157A) (see Figure 5), which is well correlated with the location of the geothermal manifestations. Usually, below 0 m of elevation, the resistivity starts to increase probably by the increment in the illite/chlorite content in the so- called mixed layer where temperatures can reach about 230°C.

3.1 Joint 1D inversion of MT and TDEM

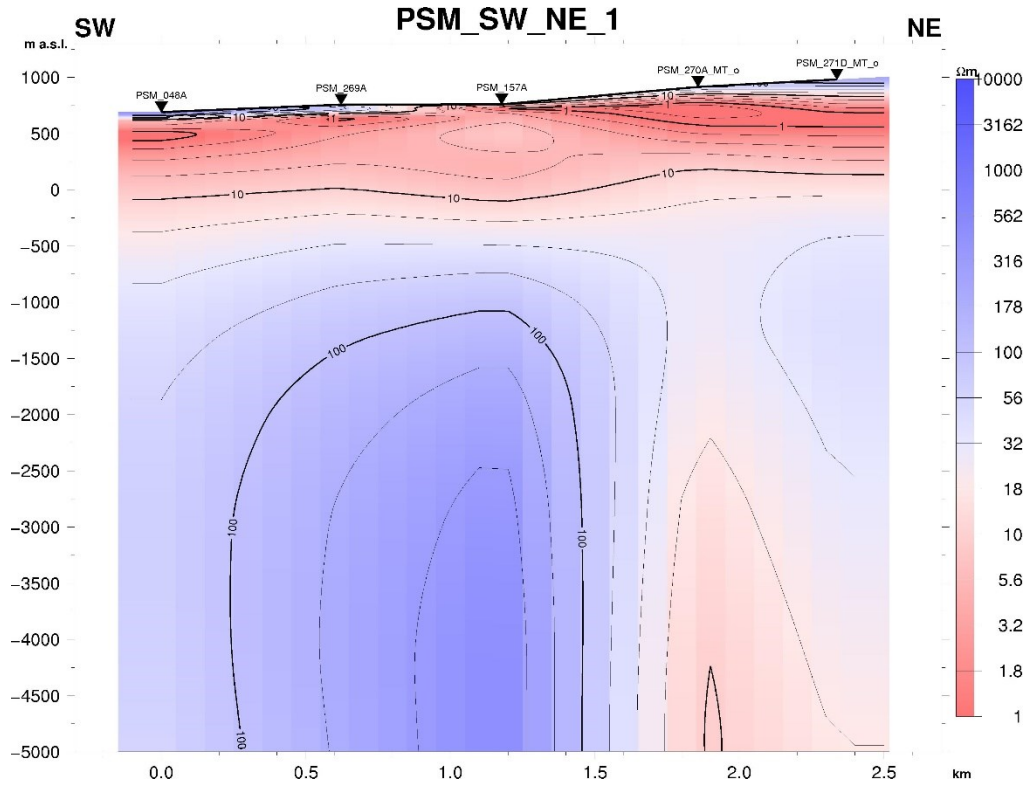


Figure 5: Result of a joint MT resistivity cross section PSM_SW_NE_01 down to 5000 m b.s.l

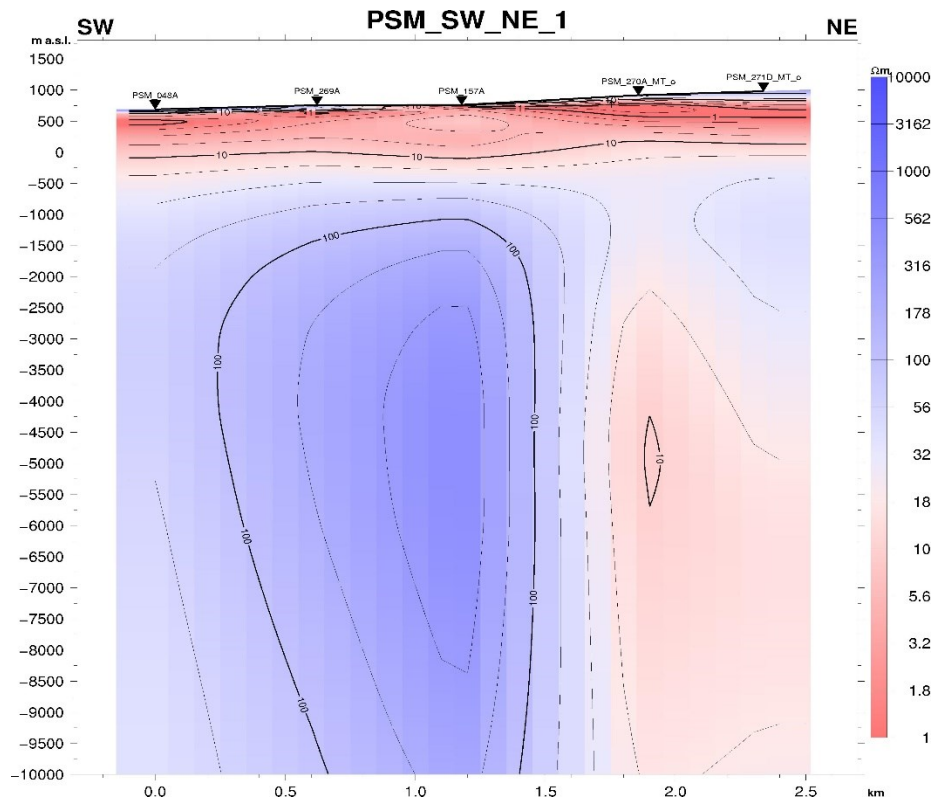


Figure 6: Result of a joint MT resistivity cross section PSM_SW_NE_01 down to 10000 m b.s.l

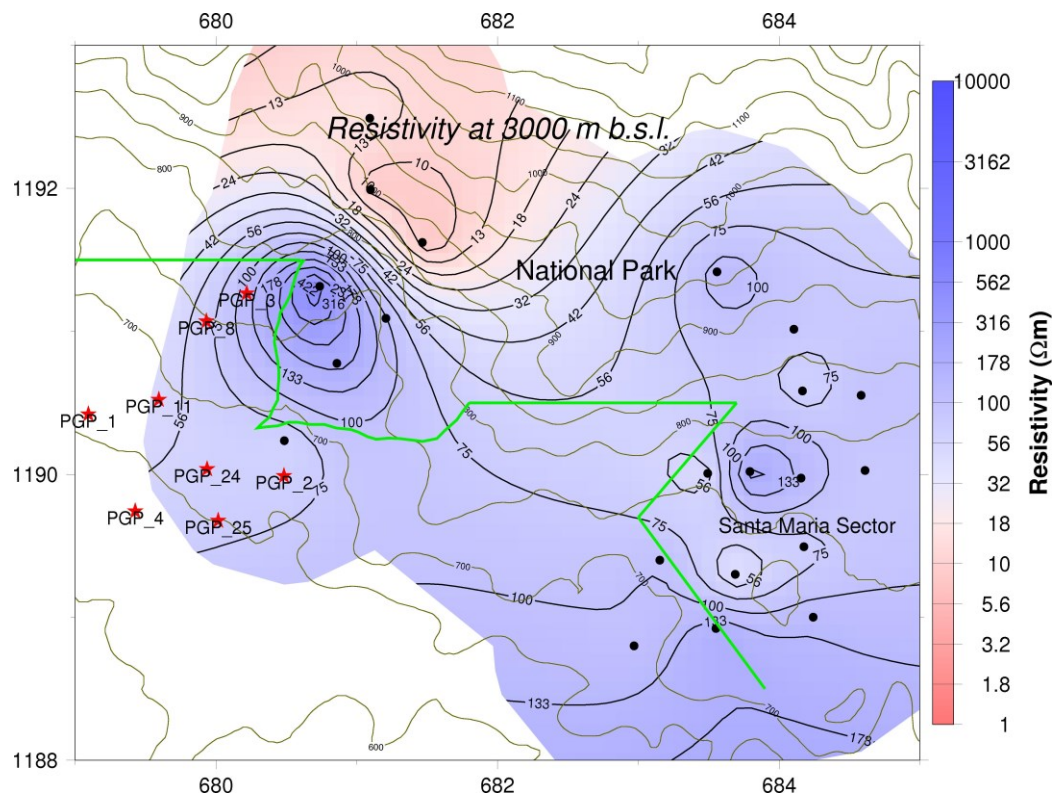


Figure 7: Resistivity depth slice map at 3000 m b.s.l. Black dots denote MT soundings. Deep wells in Las Pailas I are presented by red stars. The national park boundary is represented by a green line. UTM-Z16 (km) coordinates

4. CONCLUSIONS

A well-defined low resistivity layer is detected centred around ~500 m depth according to the cross-sections from 1D joint inversion of MT and TEM data. Its thinness varies from ~400 m to ~750 m. This shallow conductor is associated to the presence of alteration minerals like smectite and zeolites. Resistivity increases after this layer showing values between 20 Ωm and 60 Ωm at ~400 m.b.s.l, which could be interpreted as part of the smectite/illite mixed layer. A high resistivity core is found at greater depths where chlorite and epidote are dominant alteration mineral indicating possible temperatures exceeding ~240 °C.

The thickness of the conductive layer is larger toward the Santa María Sector compared to the northeast part of Las Pailas.

An important structure approximately 1 km NE from Las Pailas GF (from PGP3) aligned NW-SE is suggested due to the lateral discontinuities found in the resistivity cross sections.

The resistivity depth slice map at 3000 m b.s.l. shows in the north-eastern part of Las Pailas a deep laying (~ 3 to 6 km depth) conductor that could be associated with the heat source.

Uncertainties in the models were reduced by using constraints as the TDEM sounding data.

It is recommended to integrate all the electromagnetic data from Las Pailas GF to create a 3D inversion model and complete the static shift correction for all the MT data. This should be compared and integrated with the magnetic and gravity data.

Generating a 3D model by integrating Borinquen and Las Pailas electromagnetic data is also recommended.

REFERENCES

- Árnason, K. (1989). Central-loop transient electromagnetic sounding over a horizontally layered earth. Orkustofnun, Reykjavík, report OS-89032/JHD-06, 129 pp.
- Árnason, K. (2015). The Static Shift Problem in MT Soundings. ÍSOR, Iceland GeoSurvey. Proceedings World Geothermal Congress 2015 Melbourne, Australia, 19-25 April 2015
- Arias, O. (2002). Tectocaldera Cañas Dulces-Guachipelín, Costa Rica. Instituto Costarricense de Electricidad. [Internal report].
- Climent, A., Alvarado, G.E., Taylor, W. & Vargas, A. (2014). P.G. Las Pailas II Estudio de amenaza sísmica. - 42 págs. Instituto Costarricense de Electricidad (ICE), Costa Rica. [Internal report].

- DeMets, C. (2001). A new estimate for present-day Cocos Caribbean plate motion: Implications for slip along the Central American volcanic arc: *Geophys. Res. Letters*, 28, p. 4043–4046, doi:10.1029/2001GL013518.
- Kempton, K.A. (1997). Geologic evolution of the Rincón de la Vieja volcano complex, northwestern Costa Rica. University of Texas, PhD thesis, 159 pp.
- Phoenix Geophysics. (2015). V5 System 2000 MTU/MTU-A User Guide. Version 3.0 July 2015, Toronto, Canada.
- Sternberg, K.B., Wasburne, J.C. and Pellerin, L. (1988). Correction for the static shift in magnetotellurics using transient electromagnetic soundings. *Geophysics*, 53-11, 1459-1468.